JOURNAL OF Applied Polymer SCIENCE

Blends of Poly(3-hydroxybutyrate) with Poly(β-alanine) and Its Derivatives

Efkan Çatıker,[1] Erol Sancaktar[2]
[1]Department of Chemistry, Ordu University, Ordu 52200, Turkey
[2]Department of Polymer Engineering, University of Akron, Akron, Ohio 44325-0301
Correspondence to: E. Çatıker (E-mail: ecatiker@gmail.com)

ABSTRACT: Nanofibers and films of poly(3-hydroxybutyrate) (PHB)/nylon 3 [poly(β-alanine) (N3)], PHB/poly(α-methyl-β-alanine) (2mN3), and PHB/poly(β-methyl-β-alanine) (3mN3) blends were prepared by electrospinning and film-casting techniques, respectively. The miscibility of the blends was studied by Fourier transform infrared spectrometry, differential scanning calorimetry, thermogravimetric analysis, and X-ray diffraction (XRD). The electrospinnability of the blends was studied by scanning electron microscopy. Some characteristic IR absorption bands of the components in the blends shifted gradually with changes in the compositions. The melting temperature and decomposition temperature of PHB decreased gradually with increasing fractions of N3, 2mN3, and 3mN3. The XRD spectra of all of the blends exhibited peaks with lower intensities compared to those of the neat species. The suppression of PHB crystallinity in the blends after blending was attributed to the disruption of its crystal lattice and the prevention of recrystallization of each component by means of other components and segmental interactions between the components in the amorphous phase. Thermal, spectroscopic, and optical analyses of the polymer blends revealed that the polymers were miscible with good compatibility, and this could have improved the scaffold properties of PHB. © 2014 Wiley Periodicals, Inc. J. Appl. Polym. Sci. **2014**, *131*, 40484.

KEYWORDS: biomaterials; blends; polyamides

Received 28 October 2013; accepted 19 January 2014
DOI: 10.1002/app.40484

INTRODUCTION

Polymers have been widely used in the construction of medical devices and as tissue engineering scaffolds.[1] In biomedical applications, the criteria for selecting suitable polymers as biomaterials are based on their biocompatibility, biodegradability, hydrophilicity, molecular weight, solubility, morphological shape and structure, lubricity, surface energy, and water absorptivity. Polymeric scaffolds suitable for tissue engineering have drawn great attention because of their properties, including low density, high porosity with suitable pore size, and suitable mechanical properties. Researchers have attempted to grow skin, bone, cornea, liver, heart valve, artery, bladder, and nerve tissues and various other soft tissues[2–9] with polymeric scaffolds.

Because of their bioactive properties, natural polymers have better interactions with cells, which allow them to enhance cellular performance in biological systems. Synthetic polymers are also highly useful in biomedical fields because their properties, such as their porosity, degradation time, and mechanical characteristics, can be tailored for specific applications. Synthetic polymers are often cheaper than biologically based scaffolds, and they can be produced in large uniform quantities and have a long shelf time.

Poly(3-hydroxybutyrate) (PHB; Scheme 1) is thermoplastic biodegradable–biocompatible polyester, produced by a variety of microorganisms as an intercellular carbon and energy reserve. PHB has a high melting temperature ($T_m = 170°C$) and crystallinity. Although PHB has attracted much attention as an environmentally degradable resin to be used for various applications, it has limitations because of its brittleness (high crystallinity), narrow processability, low hydrophilicity, and low level of degradation rate compared to polylactide systems. A significant number of researchers have reported on the blending of PHB[10–21] to eliminate these limitations because it is possible to obtain polymer blends with more desirable properties through the mixture of miscible polymers. Similarly, a variety of poly(ester amide)s have been prepared by polycondensation and ring-opening polymerization to combine the favorable properties of polyesters and polyamides, and their biodegradability has been evaluated.[22–27]

Aliphatic polyamides (nylons) are generally resistant to microbial and enzymatic attacks, although some examples of degradation have been reported in the literature.[28–33] Compared to

© 2014 Wiley Periodicals, Inc.

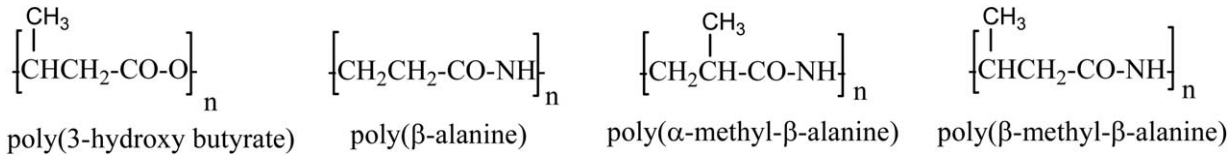

Scheme 1. Proposed components for the PHB/N3 derivatives.

aliphatic polyesters, aliphatic polyamides possess a higher thermal stability, higher modulus, and higher tensile strength. Therefore, it is reasonable to combine the favorable properties of these two classes of polymers to produce a new polymeric material possessing not only good biodegradability but also good material properties and processability.

Poly(β-alanine) (N3; Scheme 1), sometimes described as nylon 3 or polyamide 3, is a highly crystalline polymer with a high thermal and mechanical resistance. The application of N3 in different fields has already been reported,[34] such as a heat stabilizer for polyacetal resins, a textile auxiliary, and a printing agent. However, N3 is a poly(amino acid), and there was not any study on its biological activity until a few years ago.

Lee at al.[35] recently reported that some N3 copolymers support cell adhesion and have morphologies that are comparable or even superior to those achieved on positive control substrates, such as tissue-culture polystyrene and collagen-coated glass. They mainly attributed these features to the N3 backbone, which is inherently protein-mimetic. Then, Liu and coworkers published several studies on the biological activities (scaffold substrate for tissue engineering,[36] protein adsorption,[37] and antifungals[38]/antibacterials[39]) of some N3 copolymers.

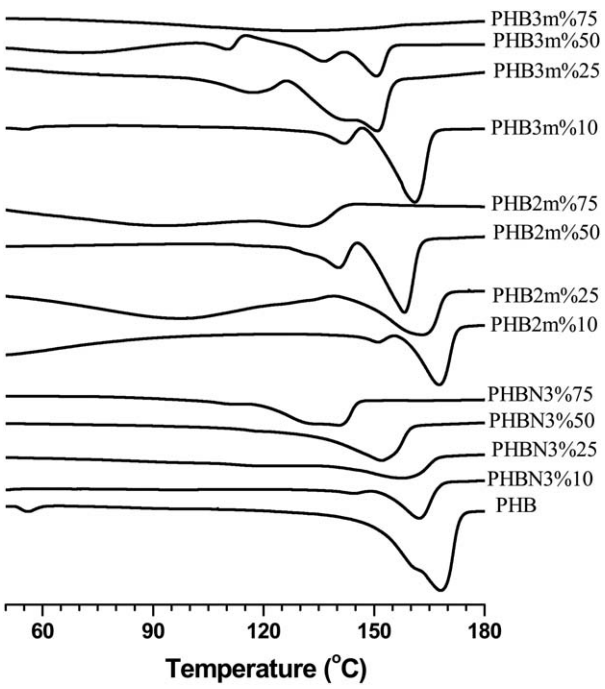

Figure 1. DSC thermograms of the neat PHB film and its blends with N3, 2mN3, and 3mN3.

Previous considerations motivated us to prepare blends of PHB with N3 and its derivatives to evaluate the miscibility of the blends for use as potential tissue engineering scaffold materials with spectroscopic [Fourier transform infrared (FTIR) spectroscopy and X-ray diffraction (XRD)], thermal [differential scanning calorimetry (DSC) and thermogravimetric analysis (TGA)], and optical [scanning electron microscopy (SEM)] techniques. We expected that these blends would exhibit better properties in the aspects of a promoted biodegardation rate, ease of processing, enhanced elasticity, improved cell attachment, and proliferation in the case of PHB/N3 blends and that its derivatives would be miscible blends. In this study, poly(α-methyl-β-alanine) and poly(β-methyl-β-alanine) are abbreviated as 2mN3 and 3mN3, respectively.

EXPERIMENTAL

Synthesis of Polymers and Blending

N3 [number-average molecular weight (M_n) = 90.000 g/mol], 2mN3 (M_n = 3.000 g/mol), and 3mN3 (M_n = 3.000 g/mol) were prepared by the hydrogen transfer polymerization of acrylamide, methacryamide, and crotonamide, respectively, with sodium *tert*-butoxide as a basic catalyst. The polymerization was carried out in a three-necked flask with continuous stirring under an argon atmosphere at 100°C for 6 h. We added potassium chloride to the reaction medium to increase the degree of polymerization by increasing the solubility of the propagating chains. Hydroquinone was added to the reaction medium to prevent possible thermally initiated vinyl polymerization. We adjusted the monomer, catalyst, KCl, and hydroquinone concentrations

Table I. Data Obtained from the DSC Curves for the Neat PHB Film and Its Blends with PBA and the PBA Derivatives

PHB/nylon	Nylon (%)	T_m (°C)	ΔH_{fusion} (J/g)	X_c (%)
PHB	0	168.1	77.6	53.2
PHB/N3	10	162.3	44.1	30.2
PHB/N3	25	158.4	33.1	22.7
PHB/N3	50	152.2	59.2	40.5
PHB/N3	75	140.8	66.9	45.8
PHB/2mN3	10	167.8	55.1	37.7
PHB/2mN3	25	165.7	55.8	38.2
PHB/2mN3	50	163.6	70.8	48.5
PHB/2mN3	75	132.3	37.2	25.5
PHB/3mN3	10	158.7	66.4	45.5
PHB/3mN3	25	150.8	58.8	40.3
PHB/3mN3	50	146.7	42.8	29.3
PHB/3mN3	75	133.2	30.0	20.5

X_c, degree of crystallinity; ΔH_{fusion}, melting enthalpy.

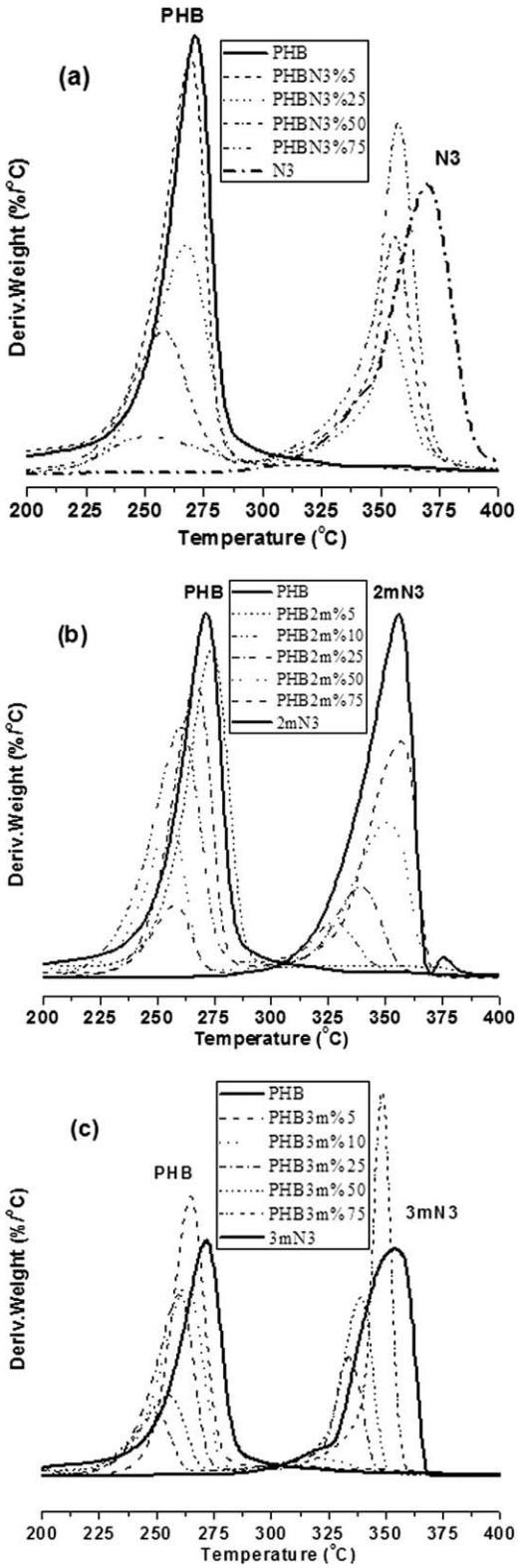

Figure 2. TGA thermograms of the neat components and blends: (a) PHB/N3, (b) PHB/2mN3, and (c) PHB/3mN3.

by following Masamoto's procedure.[40] PHB ($M_n = 100.000$ g/mol) was purchased from Goodfellow and was used without purification. The solutions of the polymer blends (10% w/v) were prepared with formic acid (Sigma, 99%). The nylon contents of the blends were in ratios of 5, 10, 25, 50, and 75 wt %. The blend solutions were stirred vigorously overnight at room temperature. The solutions were cast into Petri dishes, dried at room temperature, and stored in a vacuum oven overnight before analysis.

Table II. T_d's of the Neat Components and the Components in the Blends

PHB/nylon	Nylon (%)	T_{d1} (PHB; °C)	T_{d2} (nylon; °C)
PHB	0	272	—
PHB/N3	5	270	340
PHB/N3	25	268	354
PHB/N3	50	258	356
PHB/N3	75	252	358
N3	100	—	370
PHB/2mN3	5	274	320
PHB/2mN3	10	267	328
PHB/2mN3	25	260	339
PHB/2mN3	50	258	350
PHB/2mN3	75	259	357
2mN3		—	356
PHB/3mN3	5	265	322
PHB/3mN3	10	263	325
PHB/3mN3	25	260	334
PHB/3mN3	50	255	338
PHB/3mN3	75	247	349
3mN3	100	—	354

Blend solutions (10% w/v) in formic acid were used for the electrospinning process. The electrospinning setup consisted of a syringe pump for the injection of the polymer solution, aluminum foil as the collector of the nanofibers, and a high-voltage supply. All of the experiments were performed with a plastic syringe with a 2-mL internal volume and 0.5-mm needle diameter. The needle was connected to the high-voltage supply, and the ground electrode was connected to aluminum foil. The distance between the needle and the collector was 17 cm, and the applied voltage was 12 kV. The flow rate of the solutions was adjusted to 1 mL/h.

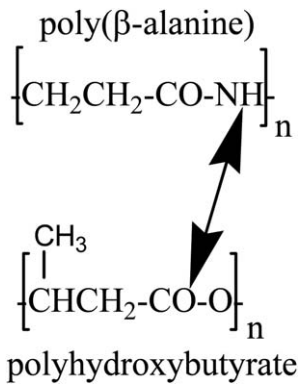

Scheme 2. Possible hydrogen bonding between PHB and N3 through the carbonyl of ester and NH of amide.

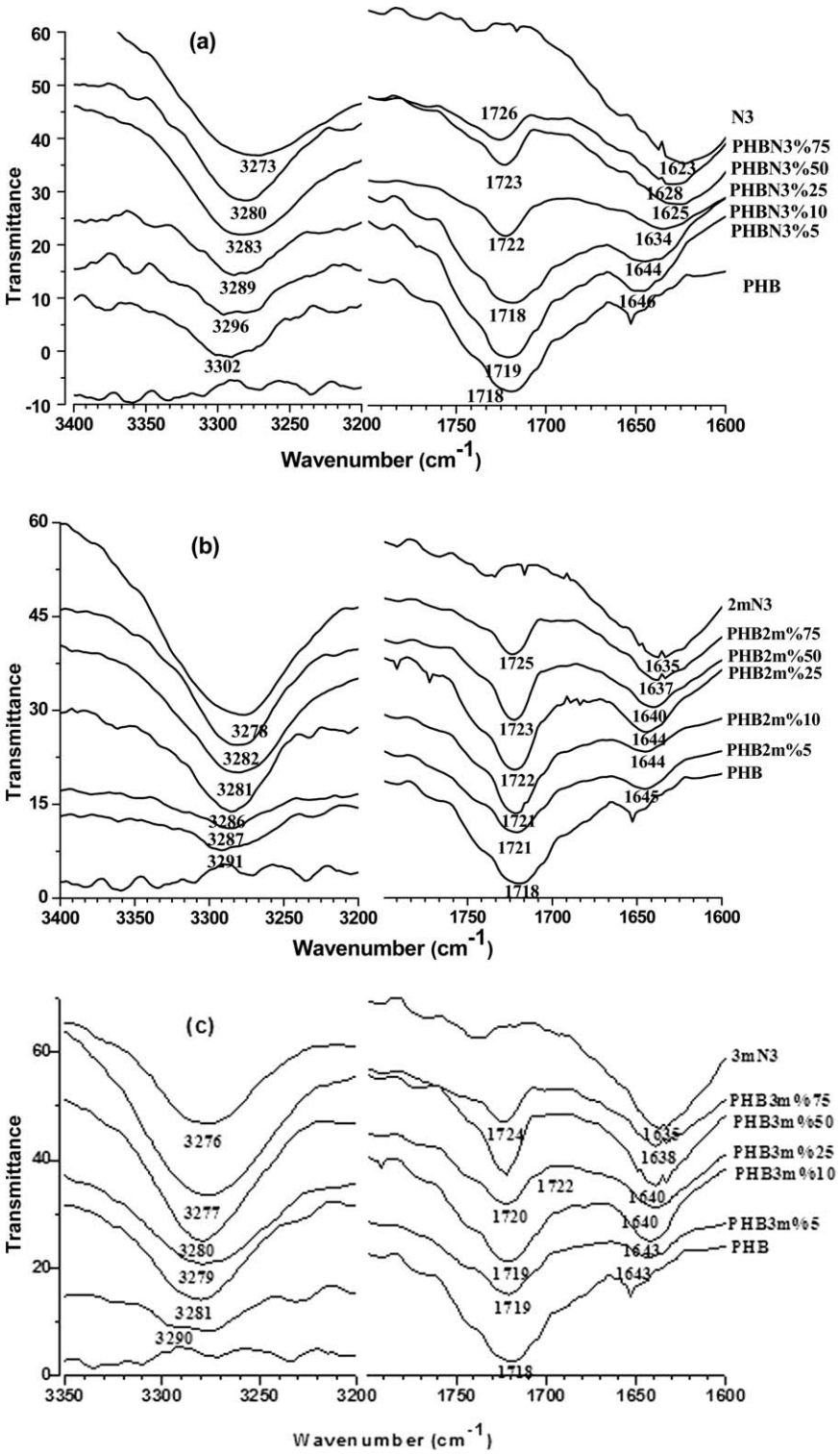

Figure 3. FTIR spectra of the (a) PHB/N3, (b) PHB/2mN3, and (c) PHB/3mN3 blends.

Characterization of the Blends

The FTIR spectra of the neat polymers and blend films were recorded at room temperature with a Nicolet 380 FTIR spectrometer. The spectra were collected over the range 4500 to 500 cm^{-1} with a resolution of 4 cm^{-1} with 32 scans. The thermal behaviors of PHB and its blends were characterized under nitrogen purge gas in the heat flux mode by a TA Instruments 2920 modulated DSC instrument. Samples of about 1–3 mg were sealed hermetically and then heated in the temperature range from −10 to 200°C at a 10°C/min rate. The instrument was operated in the conventional total heat flow mode. The T_m values were determined from the maxima

Table III. Characteristic IR Band Shifts for PHB and PBA After Blending

	Shifts increasing with nylon fraction (cm^{-1})		
	Ester carbonyl C=O stretching	Amide carbonyl C=O stretching	Amide N—H stretching
PHB/N3	1718-1726	1649-1623	3302-3273
PHB/2mN3	1718-1725	1645-1635	3291-3278
PHB/3mN3	1718-1724	1643-1635	3290-3276

of the melting peaks. The enthalpy of fusion values of the PHB components in the blends were estimated with the area of endothermic melting peak obtained by TA Instruments software (Universal Analysis 2000). TGA was performed on a TA instrument Hi-Res TGA 2950. The temperature was ramped at a heating rate of 10°C/min under nitrogen, to a temperature well above the degradation temperature of the polymers (500°C). XRD spectra of the film samples were recorded using a Bruker AXS Dimension D8 X-ray system in a range of 7–35° (2θ) using 20 kV with 5-mA current. Micrographs of the blend nanofibers (PHBN3%5, PHB2m%5, and PHB3m%5) were examined with SEM (model JEOL-7401, JEOL). Nanofiber mats were coated with a thin conductive layer of silver with a Emitack K575X sputter coater. The surface images were recorded with a voltage of 10 kV.

RESULTS AND DISCUSSION

DSC

DSC thermograms of the PHB, PHB/N3, PHB/2mN3, and PHB/3mN3 blends are shown in Figure 1. The data derived from the first heating scans of the PHB film and the PHB/N3, PHB/2mN3, and PHB/3mN3 blends are shown in Table I. The DSC curve for the pure PHB showed an endothermic T_m peak centered at 168.1°C. The T_m values of PHB in the blends decreased consistently with increasing nylon content. These decrements indicated that the PHB chains acquired enhanced mobility after blending; this led to lower T_m values. In general, a decrease in T_m in the polymeric blend could have been due to both morphological effects (a decrease in the lamellar thickness) and thermodynamic factors (suppressed cohesion forces).

The apparent enthalpy of melting for PHB decreased in the blend samples. The percentage crystallinities of PHB in the blend films were estimated by the division of the apparent melting enthalpies of PHB in the blends by the melting enthalpy of 100% PHB[41] (146 J/g). Table I shows that the relative crystallinities of PHB in all of the blend samples were lower than that in the neat PHB film. Although both the PHB and blend films were prepared with the same route (solvent, drying time, and temperature), the suppression of the percentage crystallinity of PHB in the blends may have been due to the penetration of nylons to the crystal lattice of PHB and, hence, the prevention of the recrystallization of PHB was possible due to chain entanglements. Another factor that lowered the degree of crystallinity for PHB was the difference in the molecular mobility between the PHB and nylons. The difference in the glass-transition temperature between the nylons (90–100°C) and PHB (0–5°C) influenced the degree of crystallinity of their blends. Such a result was probably due to the trapped fraction of nylon in the interlamellar amorphous regions of the PHB spherulites, which were not allowed to crystallize. Therefore, the influence of nylons on the crystallinity of PHB could be considered proof of the miscibility (compatibility) of the two polymers. The DSC results in this study revealed that the blending of the nylons with PHB suppressed the crystallinity of PHB in the blend films.

TGA

TGA of the neat components and blend films were performed to see the effects of each component on the decomposition behavior of the others. The TGA decomposition curves of the neat polymers and blends are given in Figure 2, and the corresponding data are provided in Table II. The decomposition temperatures (T_d's) of both components decreased gradually with increasing weight percentage of the other component for all of the PHB/nylon blends. Moreover, the temperature ranges for the decomposition process were narrowed. For blends with N3, 2mN3, and 3mN3, the apparent T_d values for PHB decreased by up to 20, 15, and 18°C, respectively (at a 75%

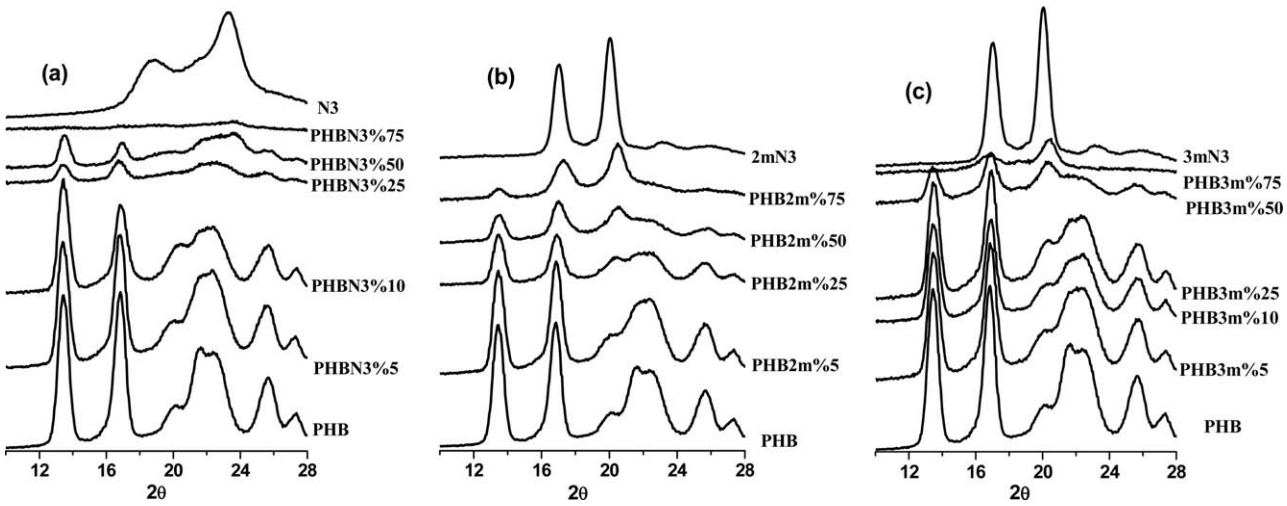

Figure 4. XRD spectra patterns of the neat components and blends: (a) PHB/N3, (b) PHB/2mN3, and (c) PHB/3mN3.

nylon level; Table II), in comparison to that of neat PHB. Similarly, the thermal T_d values of N3, 2mN3, and 3mN3 were suppressed by 30, 37, and 32°C, respectively, with increasing PHB content (Table II). This behavior indicated strong interactions (hydrogen bonding, shown in Scheme 2) between the blend components in the liquid phase immediately before decomposition. Strong segmental interactions weakened the chemical bonds in the backbones of each component; this resulted in lower T_d's and faster thermal decompositions.

FTIR Spectrometry

FTIR spectroscopy provides crucial evidence of both the crystallization and miscibility of the polymer blends. All of the polymers used in this study were highly crystalline because of the strong segmental interactions (dipole–dipole interactions in PHB and hydrogen bonding in nylons). The strong segmental interactions decreased the bonding degrees of the corresponding functional groups ($C{=}O_{amide}$, NH_{amide}, and $C{=}O_{ester}$). Consequently, the IR spectra of the neat polymers gave corresponding IR bands at lower frequencies than those in the case of the eliminated interactions. Blending the polymers may have destroyed the strong interactions between the neat polymer chains and resulted in increases in the distance between the chains, decreases in the crystallinity, and hence, increases in the chain mobility. The FTIR spectra of the blends were expected to show corresponding IR bands at higher frequencies compared to those in the neat forms because the chain mobility was enhanced. Consequently, the FTIR spectra of the PHB/N3 blends were obtained to assess any structural changes that may have occurred upon blending, as they affected the crystallinity and miscibility of the blend films. FTIR spectra of the PHB/N3 [Figure 3(a)], PHB/2mN3 [Figure 3(b)], and PHB/3mN3 [Figure 3(c)] blends with various compositions are shown in two separate graphs corresponding to 1600–1800 cm^{-1} (for CO stretching) and 3200–3400 cm^{-1} (for NH stretching) for each blend in Figure 3.

The wave-number shifts originating from the blending for characteristic amide (N—H stretching and CO carbonyl stretching) and ester (CO carbonyl stretching) bands are summarized in Table III. Table III reveals that upon blending, the wave-number value [$\nu_{C=O(ester)}$] of 1718 cm^{-1} in neat PHB shifted up to 1726 cm^{-1} with increasing N3 content. Similarly, $\nu_{C=O(ester)}$ in neat PHB shifted to 1725 cm^{-1} with 2mN3 and to 1724 cm^{-1} with 3mN3. These shifts to higher wave numbers indicated the improvement of the bond order for the corresponding group (ester CO) due to the extinction of the previous segmental interactions (here, dipole–dipole interactions).

Similarly, the $\nu_{NH(amide)}$ values in neat N3 (3273 cm^{-1}), neat 2mN3 (3278 cm^{-1}), and neat 3mN3 (3276 cm^{-1}) also shifted to higher wave numbers (3295, 3291, and 3290 cm^{-1}, respectively) with increasing PHB content; this revealed an increasing bond order for NH and, hence, the extinction of hydrogen bonding between the amide CO and amide NH.

We also observed shifts in the ν_{CO} amide band to higher wave numbers with increasing ratio of PHB in the blends. This result indicated an enhancement in the bond order for the corresponding amide CO group due to the extinction of self-associated hydrogen bonding, and it provided clear evidence for penetration of the PHB chains through the nylon crystal lattice. In all, the FTIR results support our earlier findings (Table I) that the crystallinity of the PHB/nylon blends was suppressed compared with pure components.

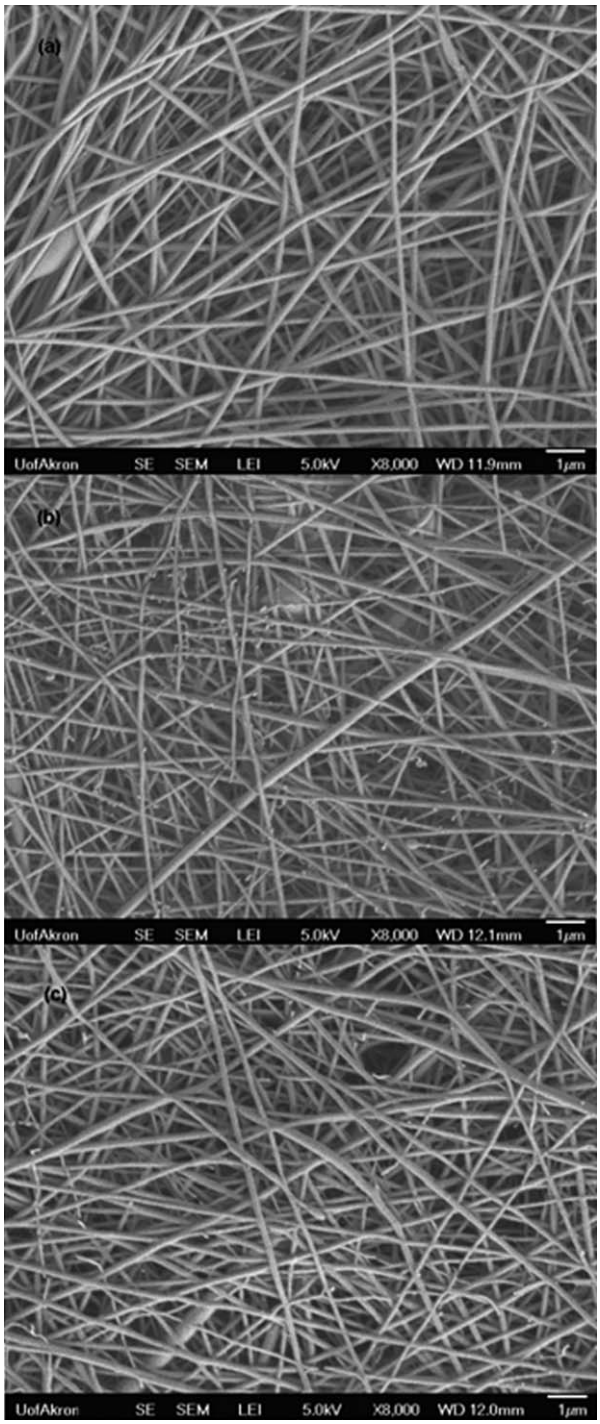

Figure 5. SEM images of (a) PHBN3%5, (b) PHB2m%5, and (c) PHB3m%5.

XRD Spectrometry

The XRD spectra patterns of the crystalline polymers could be used to extract qualitative information about the degree of

crystallinity of the polymers, blends, and composites. In this study, the XRD spectra of the neat PHB film, N3 powder, 2mN3 powder, 3mN3 powder, and blend films were obtained (Figure 4) to determine the effect of blending on the degree of crystallinity of each component.

The Miller indices of corresponding peaks were given in the spectra. The XRD spectra revealed that the diffraction intensities of the blend films were lower than those of the individual components. The sharp peaks observed in the neat PHB film spectrum diminished in intensity with increasing nylon content in the spectra for the three types of blends. Because the areas under these peaks could be used to measure the degree of crystallinity, the reduction in these areas was attributed to suppression in the degree of crystallinity for both components (PHB and nylon) upon blending. Each blend component seemed to trap the segments of the other in the amorphous phase and hinder the mobility required for crystallization. This resulted in a lower degree of crystallinity.

SEM

Subsequent to our thermal and spectroscopic investigations on the miscibilities of the PHB/N3, PHB/2mN3, and PHB/3mN3 blends, we assessed their electrospinnabilities. When the nylon contents of the blends increased (especially to >10%), the degrees of formation of the beads and bead size began to increase because of the low molecular weight of 2mN3 and 3mN3 (ca. 3000). That is why SEM images of the three types of blends with minor nylon contents (PHBN3%5, PHB2m%5 and PHB3m%5) are given here. As shown in Figure 5, the nanofibers we produced had an almost uniform structure without any sign of bead formation. The average diameter of the nanofibers seemed to be in the range 100–250 nm.

CONCLUSIONS

Thermodynamically, the formation of miscible PHB/N3 blends was favorable and was attributed to the formation of strong hydrogen bonds between the components (a decrease in enthalpy) and the suppression of high crystallinity in both the PHB and the N3 components (an increase in entropy). On the basis of this point of view, the purpose of this study was to examine the miscibility of PHB/N3 blends. Thermal, spectroscopic, and optical techniques revealed that the PHB/N3 blends were miscible in the amorphous phase. The miscibility was shown to be based mainly on the suppression of crystallinity of both components in the blends. Such a decrease in the total crystallinity should be considered a very important factor for accelerating the biodegradation of PHB, decreasing its brittleness, and improving its other relevant material properties through the adjustment of the amount of N3 to be blended.

N3 and its derivatives studied here exhibited analogous effects on the physical properties of PHB, namely, the degree of suppression in the crystallinity and electrospinnability. Thus, it is difficult to predict which of the components will offer better benefits without additional biodegradation, cytotoxicity, and cell culture studies. However, because of the low biodegradability of the nylons and current tissue scaffold applications of PHB, nanofiber blends with minor nylon content (5 and 10%) may offer benefits in the aspects of enhanced cell attachment and elasticity and controlled or promoted biodegradation rates.

REFERENCES

1. Piskin, E. J. *Biomater. Sci. Polym. Ed.* **1994**, *6*, 775.
2. Boyan, B. D.; Lohmann, C. H.; Romero, J.; Schwartz, Z. *Clin. Plast. Surg.* **1999**, *26*, 629.
3. Mayer, J.; Karamuk, E.; Akaike, T.; Wintermantel, E. *J. Controlled Release* **2000**, *64*, 81.
4. Diedwardo, C. A.; Petrosko, P.; Acarturk, T. O.; Dimilia, P. A.; Laframboise, W. A.; Johnson, P. C. *Clin. Plast. Surg.* **1999**, *26*, 647.
5. Mohammad, J.; Shenaq, J.; Rabinovsky, E.; Shenaq, S. *Plast. Reconstr. Surg.* **2000**, *105*, 660.
6. Germain, L.; Auger, F. A.; Grandbois, E.; Guignard, R.; Giasson, M.; Boisjoly, H.; Guérin, S. L. *Pathobiology* **1999**, *67*, 140.
7. Oberpenning, F.; Meng, J.; Yoo, J. J.; Atala, A. *Nat. Biotechnol.* **1999**, *17*, 149.
8. Mayer, J. E.; Shin'oka, T.; Shum-Tim, D. *Curr. Opin. Cardiol.* **1997**, *12*, 528.
9. Gaspar, A.; Moldovan, L.; Constantin, D.; Stanciuc, A. M.; Sarbu Boeti, P. M.; Efrimescu, I. C. *J. Med. Life* **2011**, *4*, 172.
10. Lotti, N.; Pizzoli, M.; Ceccorulli, G.; Scandola, M. *Polymer* **1993**, *34*, 4935.
11. Avella, M.; Martuscelli, E.; Raimo, M. *Polymer* **1993**, *34*, 3234.
12. Iriondo, P.; Iruin, J. J.; Fernandezberridi, M. *J. Polymer* **1995**, *36*, 3235.
13. Al-Rawajfeh, A. E.; Al-Salah, H. A.; Al-Rhael, I.; Jordan, *J. Chem.* **2006**, *1*, 155.
14. Greco, P.; Martuscelli, E. *Polymer* **1989**, *30*, 1475.
15. Marand, H.; Collins, M. *Polym. Prepr. Am. Chem. Soc.* **1990**, *31*, 258.
16. Al-Salah, H. A. *Polym. Bull.* **1998**, *41*, 593.
17. Asran, A. S.; Razghandi, K.; Aggarwal, N.; Michler, G. H.; Groth, T. *Biomacromolecules* **2010**, *11*, 3413.
18. Zhang, L.; Xiong, C.; Deng, X. *Polymer* **1996**, *37*, 235.
19. Ikejima, T.; Inoue, Y. *Carbohydr. Polym.* **2000**, *41*, 351.
20. Gonzalez, A.; Irirte, M.; Iriondo, P. J.; Iruin, J. *J. Polymer* **2002**, *43*, 6205.
21. El-Hadi, A.; Schnabel, R.; Straube, E.; Müller, G.; Henning, S. *Polym. Test.* **2002**, *21*,665.
22. Saotome, Y.; Miyazawa, T.; Endo, T. *Chem. Lett.* **1991**, *1*, 21.
23. Paredes, N.; Rodriguez-Galan, A.; Puiggali, J.; Pereire, C. *J. Appl. Polym. Sci.* **1998**, *69*, 1537.
24. Zhang, M.; Thomas, N. L. *Adv. Polym. Technol.* **2011**, *30*, 67.
25. Nagata, M. *Macromol. Chem. Phys.* **1999**, *200*, 2059.
26. Fan, Y.; Kobayashi, M.; Kise, H. *Polym. J.* **2000**, *32*, 817.
27. Okada, M.; Yamada, M.; Yokoe, M.; Aoi, K. *J. Appl. Polym. Sci.* **2001**, *81*, 2721.

28. Deguchi, T.; Kakezawa, M.; Nishida, T. *Appl. Environ. Microb.* **1997**, *63*, 329.
29. Fukumura, T. *Plant Cell. Physiol.* **1966**, *7*, 93.
30. Gonsalves, K. E.; Chen, X.; Wong, T. K. *J. Mater. Chem.* **1991**, *1*, 643.
31. Oppermann, F. B.; Pickartz, S.; Steinbuchel, A. *Polym. Degrad. Stab.* **1998**, *59*, 337.
32. Tomita, K.; Hayashi, N.; Ikeda, N.; Kikuchi, Y. *Polym. Degrad. Stab.* **2003**, *81*, 511.
33. Yamano, N.; Nakayama, A.; Kawasaki, N.; Yamamoto, N.; Aiba, S. *J. Polym. Environ.* **2008**, *16*, 141.
34. Yamamoto, F.; Misumi, T. *(to Asahi Chemical). U.S. Pat. 5*,015,707 (**1991**).
35. Lee, M. R.; Stahl, S. S.; Gellman, S. H.; Masters, K. S. *J. Am. Chem. Soc.* **2009**, *131*, 16779.
36. Liu, R.; Masters, K. S.; Gellman, S. H. *Biomacromolecules* **2012**, *13*, 1100.
37. Liu, R.; Vang, K. Z.; Kreeger, P. K.; Gellman, S. H.; Masters, K. S. *J. Biomed. Mater. Res. Part A* **2012**, *100*, 2750.
38. Liu, R.; Chen, X.; Hayouka, Z.; Chakraborty, S.; Falk, S. P.; Weisblum, B.; Kristyn, S.; Masters, K. S.; Gellman, S. H. *J. Am. Chem. Soc.* **2013**, *135*, 5270.
39. Chakraborty, S.; Liu, R.; Lemke, J. J.; Hayouka, Z.; Welch, R. A.; Weisblum, B.; Masters, K. S.; Gellman, S. H. *ACS Macro Lett.* **2013**, *2*, 753.
40. Masamoto, J.; Sasguri, K.; Ohizumi, C.; Kobayashi, H. *J. Polym. Sci.* **1970**, *8*, 1703.
41. Barham, P. J.; Keller, A.; Otun, E. L.; Holmes, P. A. *J. Mater. Sci.* **1984**, *19*, 2781.